Cooperative synapse formation in the neocortex

Tarec Fares and Armen Stepanyants[1]

Department of Physics and Center for Interdisciplinary Research on Complex Systems, Northeastern University, Boston, MA 02115

Edited by Eve Marder, Brandeis University, Waltham, MA, and approved August 4, 2009 (received for review January 2, 2009)

Neuron morphology plays an important role in defining synaptic connectivity. Clearly, only pairs of neurons with closely positioned axonal and dendritic branches can be synaptically coupled. For excitatory neurons in the cerebral cortex, such axo-dendritic oppositions, termed potential synapses, must be bridged by dendritic spines to form synaptic connections. To explore the rules by which synaptic connections are formed within the constraints imposed by neuron morphology, we compared the distributions of the numbers of actual and potential synapses between pre- and postsynaptic neurons forming different laminar projections in rat barrel cortex. Quantitative comparison explicitly ruled out the hypothesis that individual synapses between neurons are formed independently of each other. Instead, the data are consistent with a cooperative scheme of synapse formation where multiple-synaptic connections between neurons are stabilized while neurons that do not establish a critical number of synapses are not likely to remain synaptically coupled.

barrel cortex | connectivity | morphology | potential synapse | pyramidal cell

Our understanding of the rules governing synaptic connectivity in the brain is hindered by the complexity of neuron morphology. To circumvent this problem, it is often necessary to explicitly account for the shapes of axonal and dendritic arbors in the analysis of synaptic connectivity (see e.g., refs. 1–4). In the cerebral cortex, the majority of synaptic connections between excitatory neurons are made on dendritic spines (5). Therefore, individual synapses between neurons occur in places where axonal branches of the presynaptic neuron are located within spine reach from the dendritic branches of the postsynaptic cell. Such axo-dendritic oppositions are termed potential synapses (6, 7). Because in the adult cerebral cortex axonal and dendritic arbors of excitatory neurons form an extremely stable scaffold (8–11), the resulting matrix of potential synapses is stable as well (see however refs. 11–13, where small, layer specific changes in terminal axonal and dendritic branches were observed). What is more, due to the stereotypic morphologies of dendritic and local axonal arbors of cortical neurons (same species, brain region, layer, etc.) (14), the matrix of potential synapses is expected to be similar among different brains (6, 15). This matrix constrains possible connectivity patterns in the adult brain and provides the main avenue for the formation of new synaptic connections. A potential synapse can be converted into an actual synapse if the gap between the pre- and the postsynaptic branches is bridged by a dendritic spine.

In this study, we examine the rules of excitatory connectivity within the constraints imposed by the morphologies of neurons, i.e., within the matrix of potential synapses. Different connectivity patterns can be built within this matrix by converting different sets of potential synapses into actual. However, not all such connectivity patterns are biologically plausible since even within the matrix of potential synapses, synaptic connectivity is built according to specific rules (2). We ask and attempt to answer 2 questions. Are the individual synaptic connections between potentially connected neurons established independently of each other? If not, what are the possible rules governing synaptic connectivity within the potential connectivity matrix?

Results

Actual and Potential Synapses Between Nearby Neurons. Pairs of excitatory neurons in the cerebral cortex typically share several potential synapses whenever there is a significant overlap of their axonal and dendritic arbors (Fig. 1*A*). This is true for most nearby excitatory neuron pairs and for some local interlaminar projections in the neocortex (see e.g., refs. 2, 6, 15–20). In particular, in rat barrel cortex, neuron pairs forming local (separated by less than 50 μm laterally) layer 4 to layer 2/3 (L4→L2/3), L5→L5, and L4→L4 projections are known to have numerous potential synapses (1, 3). Hence, it is not surprising that the numbers of actual synapses between such synaptically coupled neurons are numerous as well (21–23) (Fig. 1 *B–D*).

What comes to us as a surprise is that the distributions of actual synapse numbers between synaptically coupled neurons forming these projections are highly tuned; i.e., the ratios between variance and mean (the Fano factor) of these distributions are significantly less than 1: 0.060 for L4→L2/3, 0.21 for L5→L5, and 0.31 for L4→L4 projections. In particular, these distributions are many fold less variable than the corresponding distributions of potential synapse numbers (Fig. 1 *B–D*) for which the Fano factors are greater than 1: 2.0, 3.2, and 2.2 respectively. This suggests that individual actual synapses between pre- and postsynaptic neurons may have been chosen from the potential synapses not randomly, e.g., not independently of each other. Is it possible that a cell can somehow regulate the numbers of synapses made with its individual synaptic partners? We examined this idea quantitatively by analyzing experimentally observed numbers of actual synapses between neurons (21–23) together with the dataset of neuron morphologies reconstructed in 3D (1) [obtained from http://NeuroMorpho.org (24)].

Model of Independent Synapse Formation. Synaptic connectivity between nearby neurons or neurons forming local interlaminar projections is very sparse; i.e., the probabilities of finding such connected neurons are low [0.03–0.3 (25)]. Despite this sparseness, synaptically coupled neurons are typically interconnected with several synapses (21–23). Clearly, if actual synapses were formed completely randomly at the potential synaptic sites, low probabilities of connection would entail small (1 or sometimes 2) numbers of actual synapses between synaptically coupled neurons (2), which is inconsistent with the experimental evidence. To reconcile the numbers, one could consider the fact that neurons, even in the same small cortical region, may differ in their functional properties. Hence, a given neuron may only connect to some of its (synaptically compatible) potential partners, establishing individual synaptic connections with them probabilistically and independently of one another. As a result, it may be possible to have a low probability of connection on the one hand and a high connectivity between synaptically coupled neurons on the other.

Author contributions: A.S. designed research; T.F. and A.S. performed research; T.F. and A.S. analyzed data; and T.F. and A.S. wrote the paper.

The authors declare no conflict of interest.

This article is a PNAS Direct Submission.

Freely available online through the PNAS open access option.

[1]To whom correspondence should be addressed. E-mail: a.stepanyants@neu.edu.

This article contains supporting information online at www.pnas.org/cgi/content/full/0813265106/DCSupplemental.

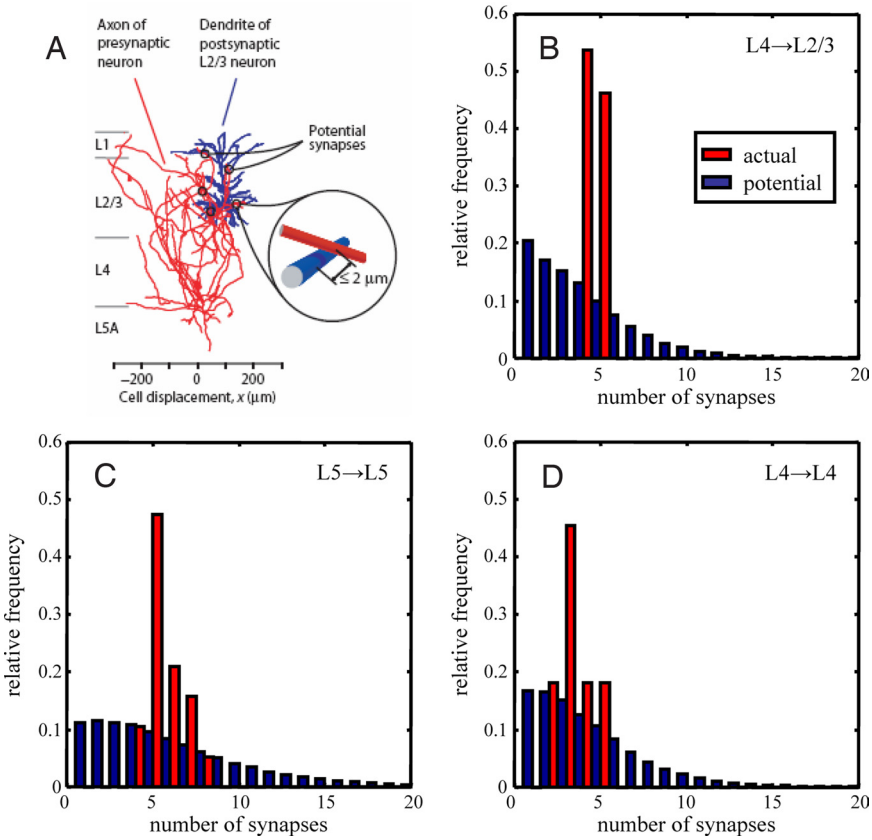

Fig. 1. Potential and actual synapses. (*A*) 3D reconstructions of a layer 4 spiny stellate cell axon (red) and a layer 2/3 pyramidal cell dendrite (blue) from rat barrel cortex. Potential synapses between the arbors are shown with small black circles. Adopted from figure 3a in ref. 1. (*B*) Distribution of the numbers of potential synapses (blue) and distribution of the numbers of actual synapses for synaptically coupled neurons (red) forming local L4→L2/3 projection. (*C*) Same for pairs of nearby neurons in L5. (*D*) Same for pairs of nearby neurons in L4.

To examine this idea quantitatively, we simulated the model of independent synapse formation in which individual synapses between synaptically compatible neurons are formed at the potential synaptic locations probabilistically and independently of each other (see *Materials and Methods* for details). We used a Monte Carlo procedure and generated the distributions of actual synapse numbers for pairs of synaptically compatible neurons. To this end, we first randomly selected reconstructed neuron pairs, and for every pair identified the potential synaptic sites with a computer search algorithm. Next, we randomly converted individual potential synapses into actual with a fixed probability p, which was assumed to be independent of synaptic locations on axonal and dendritic arbors, as well as their cortical positions (*SI Text* and Fig. S1).

In result, for different values of the parameter p, we generated the distributions of actual synapse numbers, which take into account the morphological characteristics of neurons belonging to different cortical layers (Fig. 2). For every value of the parameter p and for all of the projections, the generated and the experimental distributions of synapse numbers are statistically different (P value $\leq 10^{-5}$ for L4→L2/3 and L5→L5, and ≤ 0.002 for L4→L4, see *SI Text*). We conclude that the idea of independent synapse formation is irreconcilable with the experimental data.

Cooperative Synapse Formation Model. To reconcile the experimental observations of highly tuned connectivity between synaptically coupled neurons with broadly distributed potential synapse numbers, we next explored the possibility of cooperative (not independent) synapse formation. We hypothesized that, to be synaptically coupled, neurons must be connected with greater than some critical number of synapses. To model such cooperative synapse formation, we introduced a monotonically increasing function, $f(N_s)$, which is the probability that a cell pair, initially connected with N_s synapses, will remain synaptically coupled. Specifically, we used a two-parameter sigmoidal function,

$$f(N_s) = \frac{1}{1 + \exp\left[-\frac{4}{\Delta}(N_s - N_s^c)\right]}, \qquad [1]$$

where $N_s^c > 0$ and $\Delta > 0$ specify the position of the inflection point and the inverse slope (cotangent) at that position. Because

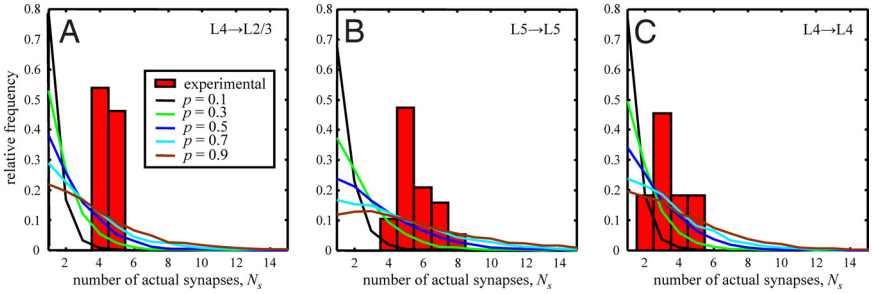

Fig. 2. Individual synapses between neurons are not formed independently of each other. (*A*) Experimental distribution of the numbers of actual synapses (red bars) between synaptically coupled neurons forming local L4→L2/3 projection. Individual lines show the distributions of actual synapse numbers obtained from the model of independent synapse formation for different values of the parameter p. (*B*) Same for pairs of nearby neurons in L5. (*C*) Same for pairs of nearby neurons in L4.

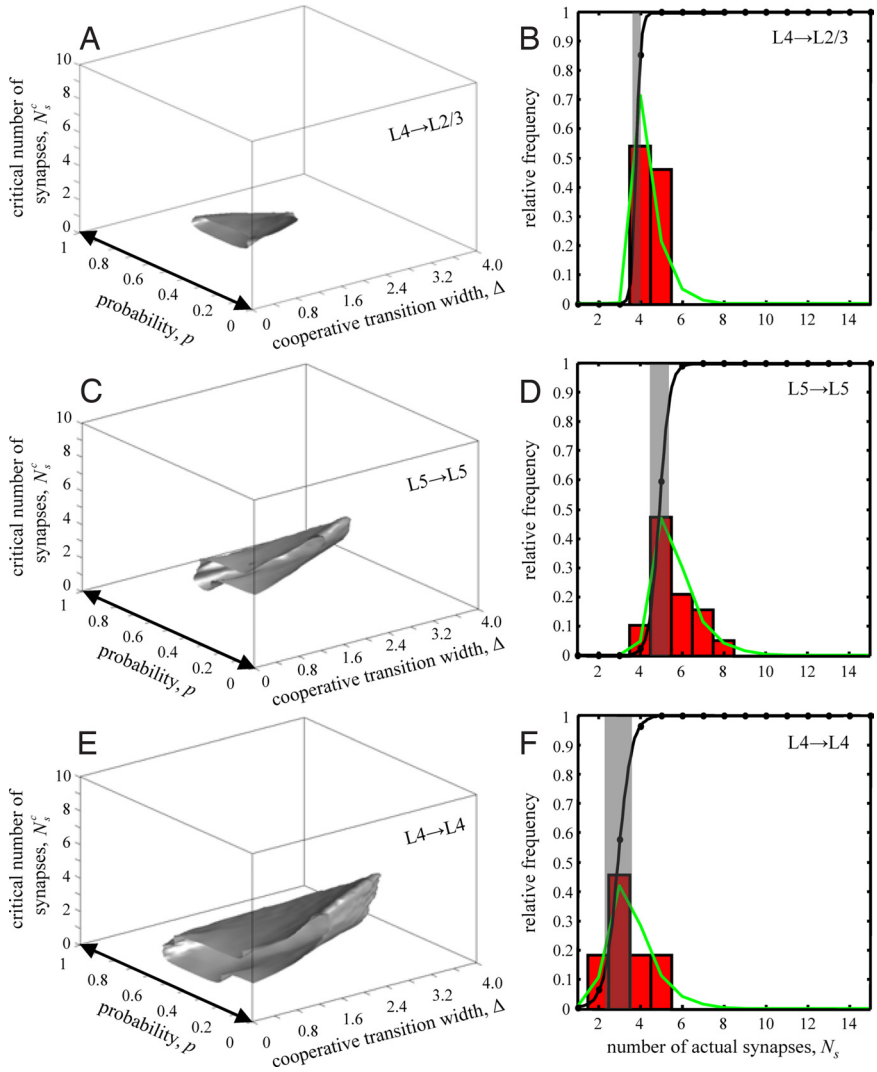

Fig. 3. Synapses between neurons are formed in a cooperative manner. (*A*) 95% confidence region for the model parameters p, N_s^c, and Δ for local L4→L2/3 projection. Left-right arrow on the p-axis indicates the parameter region of the independent synapse formation model. (*B*) Bar plot shows the experimental distribution of the numbers of actual synapses for local L4→L2/3 projection. The distribution of actual synapse numbers obtained from the model for the average values of the parameters p, N_s^c, and Δ is shown with a green line. Function f (N_s) for this parameter values is shown in black. Gray strip of width Δ, centered at N_s^c, marks the cooperative transition window. (*C* and *D*) Same for pairs of nearby neurons in L5. (*E* and *F*) Same for pairs of nearby neurons in L4.

N_s^c marks the position of the cooperative transition, we refer to this parameter as the critical number of synapses. The parameter Δ controls the sharpness of the cooperative transition. For example, in the transition window of width Δ centered at N_s^c the value of $f(N_s)$ changes from 0.12 to 0.88. For this reason, Δ is referred to as the width of the cooperative transition. Similar to the model of independent synapse formation, individual potential synapses between neurons are transformed into actual synapses with a fixed probability p. However, in this model the sigmoidal function makes it less likely that neurons coupled with low numbers of synapses will retain their connections.

Exploring the space of the model parameters p, N_s^c, and Δ, we identified parameter values for which the model distributions of synapse numbers were not significantly different from the experimental distributions (see *SI Text* for details). Fig. 3 *A*, *C*, and *E* show surfaces that enclose the 95% confidence regions for the values of p, N_s^c, and Δ. The confidence regions for the 3 projections are similar in shape but differ in size. Because there are parameter values that are common to all three 95% confidence regions, it is possible that all three projections are governed by the same set of parameters. In the limit of small values of N_s^c and Δ (p-axis in Fig. 3 *A*, *C*, and *E*), the cooperativity function, $f(N_s)$, approaches 1 for all nonzero numbers of synapses, and the model transforms into the model of independent synapse formation. Fig. 3 *A*, *C*, and *E* clearly show that this parameter regime (left-right arrows) falls outside the 95% confidence regions, again illustrating that the model of independent synapse formation is inconsistent with the experimental data.

Table 1 contains the average values of the model parameters p, N_s^c, and Δ, as well as their 95% confidence intervals. The most

Table 1. Results of the cooperative synapse formation model

Projection	p	N_s^c	Δ	P_{con}
L4→L2/3	0.18 ± 0.090 (0.025–0.40)	3.8 ± 0.38 (3.1–5.3)	0.47 ± 0.28 (0.10–1.2)	0.020 ± 0.023 (0–0.11)
L5→L5	0.19 ± 0.10 (0.025–0.40)	4.9 ± 0.73 (3.1–7.6)	0.98 ± 0.58 (0.10–2.3)	0.040 ± 0.051 (0–0.25)
L4→L4	0.27 ± 0.13 (0.025–0.60)	2.9 ± 0.90 (1.1–6.4)	1.3 ± 0.79 (0.10–3.5)	0.16 ± 0.15 (0–0.62)

Numerical values are shown in the mean ± SD (95% confidence interval) format.

salient feature of the results is that the width of the cooperative transition, Δ, is on the order of a single synapse for all projections. Hence, the cooperative transitions are extremely sharp. The high degree of cooperativity becomes evident from the inspection of functions $f(N_s)$ in Fig. 3 *B*, *D*, and *F* (black lines), where these functions were plotted for the average values of N_s^c and Δ. In these figures, gray windows of widths Δ, centered at the critical numbers of synapses, N_s^c, demarcate the cooperative transition regions. At $N_s = N_s^c$, the probability for a neuron pair to maintain its connection is 0.5. A single synapse above or below the critical number of synapses transforms this probability into nearly one or zero. In other words, a single synapse in excess of the critical number of synapses is sufficient to stabilize the connection, and, conversely, a single synapse below the critical value will result in the connection loss. Hence, cells appear to have a mechanism for effectively thresholding the numbers of synapses formed with their individual synaptic partners.

Knowing the values of the model parameters p, N_s^c, and Δ makes it possible to calculate the probability, P_{con}, that a pair of neurons, randomly selected from one of the considered projections, is synaptically coupled. For all of the projections, the values of P_{con} calculated based on the cooperative model (see Table 1) are in good agreement with the reported experimental probabilities of connection, which are 0.03 for L4→L2/3, 0.10 for L5→L5, and 0.20–0.30 for L4→L4 projections (21–23). These results provide independent evidence in support of the cooperative synapse formation model.

Discussion

The results of this study are 2-fold. First, we showed that the idea of independent synapse formation between pre- and postsynaptic neurons is inconsistent with the experimental datasets of neuron morphology and synaptic connectivity. Second, we proposed a cooperative model of synapse formation, which led to a good agreement with the experimentally observed distributions of synapse numbers and the probabilities of finding synaptically coupled pairs of neurons. Our numerical results suggest that cells effectively threshold the numbers of synapses formed with their individual synaptic partners. Strong multiple-synaptic connections, which exceed the critical number of synapses, are stabilized, whereas weak connections are degraded.

Potential connectivity in this study was inferred by putting together neurons reconstructed from different animals. As a result, we disregarded correlations in the shapes of axonal and dendritic arbors, which may be present in vivo. For example, if positions of axonal and dendritic branches of synaptically connected neurons were positively correlated in space, then our method would systematically underestimate the true numbers of potential synapses and may create a bias toward cooperativity. Positive spatial correlations had been observed between axons of inhibitory neurons and their postsynaptic targets, but not for the general population of excitatory cells (16). Correlations are likely to exist between ontogenetic radial clones of excitatory cells (26) whose main axons and apical dendrites are known to follow the direction of the parent radial glial cell. As a result, such sister cells may establish higher numbers of potential synapses in comparison to other neuron pairs with similar cortical positions. This supposition is consistent with the fact that the probability of connection for these pairs is several fold higher compared to their neighbors. However, because sister cells comprise only a small fraction of all pairs forming the considered projections, their influence on our results is negligible.

As shown in Fig. 1, projections with significantly overlapping axonal and dendritic arbors (few potential synapses on average) have broad distributions of potential synapse numbers. These distributions typically have Fano factors of greater than 1 (2–3 in this study). If potential synapses were converted into actual synapses noncooperatively, one would expect the Fano factor for actual synapses to be greater than 1 as well. Hence, a low (less than 1) Fano factor for actual synapses may be used as an indicator of cooperativity. This is the case for several inter and intralaminar projections where these factors are: 0.060 for L4→L2/3 (22), 0.21, 0.42, and 0.89 for L5→L5 (23, 27, 28), 0.31 for L4→L4 (21), and 0.34 for L4→L5 (29). As a rigorous proof of cooperativity, however, it is necessary to reconstruct neuronal arbors forming the projections and repeat the analysis presented in this study.

It is important to mention that, because our analysis is based on very local laminar circuits (lateral separation between neurons is less than 50 μm), it is not clear if the mechanism of cooperative synapse formation can be generalized to cortical circuits of a longer-range. In fact, the overwhelming majority of synapses received by postsynaptic cells are mediated by these longer-range connections. In cat V1, for example, 97% of synapses received by an average postsynaptic excitatory neuron originate from presynaptic neurons that are located beyond the 50 μm range in the cortical plane (30). These longer-range projections may include inter- and intra-areal connections, feedback from higher cortical areas, and interhemispheric projections. Often, these projections are mediated by sparse axons, which pass through dendritic arbors' territories without branching on the way to their ultimate target regions. Such unbranched axon segments may establish single potential, and hence actual, synapses with their postsynaptic neurons, exhibiting no cooperativity.

What could be the biological advantage of connecting neurons with multiple synapses, as opposed to having monosynaptic connections of equivalent strengths? A theoretical answer to these questions lies in the fact that for noise-limited information transmission (31) it is more cost-effective to connect pre- and postsynaptic cells with several small, although noisy synapses, rather than a single, more reliable synapse of an equivalent strength. Mechanistically, it is likely that individual synapses between potentially connected axonal and dendritic branches are established according to some local molecular or activity dependent rules (2). Hence, synaptically compatible cells will attempt to convert all their potential synapses into actual, leading to multiple-synaptic connections between them.

The proposed idea of cooperative synapse formation is compatible with competitive interactions between motor axons observed at developing neuromuscular junction (32). In that system, as a result of competition, one axon withdraws from the postsynaptic site, while the winner typically extends to occupy the abandoned territory. One difference between the systems is that motor axons appear to be competing for targets localized in space; whereas in the neocortex, individual axons are competing for the connection with the postsynaptic cell through synapses that are distributed over the dendritic arbor. Cooperativity in synapse formation may be constrained by the homeostatic regulation of connectivity. Similar to the morphological homeostatic regulation of spine sizes and densities (33) or the regulation of individual branches within an arbor (34), the overall number of synapses on a dendritic arbor may be regulated as well (8). In this case, cooperative synapse formation with one cell will be accompanied with the elimination of existing synapses with other cells and may lead to loss of the connections in which the number of synapses drops below critical.

Finally, we note that to implement the proposed thresholding mechanism, cells must have information about the numbers of synaptic connections with their individual synaptic partners. This seems incredible given the fact that an average excitatory cell in rat barrel cortex forms thousands of synaptic connections with hundreds of neurons. Then what could be the biologically plausible mechanism of cooperative synapse formation? The answer is not entirely clear. It has been suggested that the initial dendritic spine or filopodium outgrowth may be directed (35), induced, for example, by the coincident pre- and postsynaptic neuron activity (36). Within minutes after the onset of activity, new spines will grow and bridge the potential synaptic gaps between the pre- and postsyn-

aptic neurons, establishing initial contacts. It will, however, take many hours before these contacts are transformed into synapses as judged by ultrastructural criteria (35). It is plausible that during, or shortly after, this period of spine maturation, when the synapses become functional, the mechanism of cooperativity begins to work. Since the number of synapses between neurons is positively correlated with the connection strength (2, 21–23), this mechanism may be similar to those of long-term potentiation and depression (37–41). Connections that are mediated by large numbers of newly formed functional synapses may be maintained because the activation of presynaptic cells in these neuron pairs is more likely to trigger postsynaptic responses. Conversely, connections between neurons that have smaller than the critical number of synapses may not be strong enough to propagate neural activity effectively and are eliminated. This supposition is reasonable for L4→L4 projection where unitary excitatory postsynaptic potentials had been shown to elicit action potentials in spiny stellate neurons in the in vitro slice preparation (21). For L4→L2/3 and L5→L5 projections in the slice, it had been estimated that simultaneous activation of 5 to 100 (depending on connection strength and reliability) presynaptic neurons is needed to bring the postsynaptic cell to the threshold of firing (22, 23). However, because of tissue slicing artifacts (30) these numbers in vivo are expected to be significantly lower. Moreover, due to a different electro-physiological state of the neural network in vivo (42), the minimum number of simultaneously active presynaptic neurons needed to fire the postsynaptic cell may be lower yet.

Materials and Methods

Experimental Procedures. The results of this study are based on the combined analysis of datasets of neuron morphology and synaptic connectivity in rat barrel cortex. The dataset of 3D neuron morphology used in this work was originally reconstructed in the context of the Shepherd et al. study (1). This dataset was obtained from http://NeuroMorpho.org (24). Because the experimental procedures related to this dataset were previously described (1), in the following we only provide a brief summary of facts that are relevant to our work. Young adult Sprague-Dawley rats (26–36 days postnatal) were used in the experiment. Three hundred micrometer-thick slices of barrel cortex were cut perpendicular to barrel rows. Excitatory cells located 50 to 100 μm (mean of 78 μm) below slice surface were labeled with biocytin and reconstructed in 3D with Neurolucida system (MicroBrightField Inc.). In total, 13 pyramidal cells from L2/3, 13 spiny stellate, and 13 pyramidal cells from L4, and 23 pyramidal cells from L5A were reconstructed from barrel (33 cells) and septum (29 cells) related columns. All reconstructions were corrected for tissue shrinkage and conformed to the template of a barrel cortical slice. This was an essential step, because for the analysis of potential connectivity it is typically necessary to put together neurons reconstructed from different brains.

The distributions of synapse numbers for pairs of synaptically coupled neurons forming L4→L2/3, L5→L5, and L4→L4 projections were measured in a series of studies performed in the Sakmann group (21–23). In these experiments, 300–400 μm thick cortical slices were obtained from juvenile (12–23 days postnatal) Wistar rats. The L4→L2/3 (13 neuron pairs in the barrel column) (22) and L4→L4 (11 barrel related neuron pairs) (21) projections were studied in rat barrel cortex and the L5→L5 (19 thick tufted pyramidal cell pairs) (23) projection in rat somatosensory cortex. Dual whole-cell recordings were used to identify synaptically coupled neurons. Such neurons were typically separated by no more than 50 μm in the direction along the cortical surface and were located up to 120 μm deep in the slice (80 μm on average). The neurons were labeled with biocytin and their putative synaptic contacts were identified as close oppositions of a bouton and dendrite in the same focal plane. To confirm that the putative synapses, detected with light microscopy, were indeed synaptic contacts, a subset of them was analyzed with serial electron microscopy. Since more than 80% of putative synapses were confirmed at the electron microscopy level (22, 23, 43), light microscopic predictions were deemed accurate. However, very small synapses, or synapses hidden by thick dendrites, may have been omitted, which would result in an underestimation of synapse numbers. We do not expect small underestimations to affect the conclusions of this study since larger synapse numbers would lead to even greater differences between the distributions of actual and potential synapse numbers.

The Distribution of Potential Synapse Numbers. In this study, a potential synapse is defined as an opposition between axonal and dendritic branches of 2 neurons, where the distance between the branch centerlines is less than $s = 2$ μm. Assumptions and approximations related to the concept of the potential synapse, as well as different definitions of potential connectivity, were previously described (6, 44). According to the definition used in this study, one potential synapse at most can exist between a pair of axonal and dendritic branches, independent of their lengths and relative layout. A branch here is defined as a neuron process connecting a cell body or a bifurcation point to a successive bifurcation or an end point. The above constraint is necessary to disambiguate situations where potentially connected axonal and dendritic branches ran in parallel over long distances. Because this is a rare occurrence for cortical excitatory neurons, the numbers of potential synapses calculated according to this definition are in good agreement with other estimates (see e.g., figure 3C in ref. 1). The value of $s = 2$ μm was chosen for the definition of a potential synapse, as it corresponds to the average distance between centerlines of synaptically connected axonal and dendritic branches (7), i.e., this value is roughly equal to the sum of the average dendritic spine length, the average dendritic branch radius, and the average axonal bouton radius. Although the average number of potential synapses between cells scales linearly with s (6, 16), and hence the shape of the distribution of potential synapse numbers is also dependent on s (Fig. S2), the main results of this study are not very sensitive to particular values of this parameter. This point is illustrated in Fig. S3, where all of the results were replicated for $s = 1.5$ μm and $s = 2.5$ μm.

The numbers of potential synapses were calculated for all pairs of neurons by using a computer search algorithm (15) which finds and counts close oppositions between axonal and dendritic branches in the arbors' overlap region. As the number of potential synapses is very sensitive to exact placement of individual branches within the arbors' overlap region, 1,000 different realizations of potential connectivity were considered for each neuron pair. This was done by randomly shifting the arbors around their original positions in the slice template of rat barrel cortex. Random shifts of the neurons were performed in the plane of the slice and were confined to 20 μm square regions surrounding the neurons' original positions. Because axonal arbors of the neurons were significantly truncated due to tissue slicing, the neurons were not moved in the direction perpendicular to the slice surface. Likewise, the neurons were not shifted over large distances in the plane of the slice as the shapes of axonal and dendritic arbors depend on neuron's positions with respect to the laminar and barrel boundaries.

To emulate the conditions of the Sakmann lab experiments (21–23), only neuron pairs with separations of no more than 50 μm in the direction along the cortical surface (in the plane of the slice) were considered. This restriction resulted in 70 neuron pairs for L4→L2/3 projection, 104 pairs for L5→L5 projection, and 116 pairs for L4→L4 projection. For each projection, the distribution of the numbers of potential synapses was obtained by pooling the 1,000 potential synapse numbers generated for each neuron pair (Fig. 1 *B–D*). The results of this study are based on the morphologies of neurons reconstructed from barrel and septum-related columns (1). Because dendritic and local axonal morphologies of neurons in these regions are similar (1), the distributions of potential synapse numbers for the considered projections were also similar in the barrel and septum-related columns. We separately analyzed barrel and septum related projections and because no significant differences in the results were detected, these projections were pooled.

Model of Independent Synapse Formation. In the independent synapse formation model (IM), cortical cells forming a particular projection may differ in their functional properties which determine their preferences in establishing synaptic connections with each other. Some pairs of cells would couple synaptically when given the opportunity. Such pairs are referred to as synaptically compatible. The probability that a randomly chosen pair of neurons is synaptically compatible is denoted with κ.

A synaptically compatible pair of neurons has a chance of establishing a synaptic connection only if it is potentially connected. These neuron pairs convert their individual potential synapses into actual synapses according to a fixed probability, p (see *SI Text* for a test of this assumption). Hence, the probability that a pair of these cells will establish precisely N_s actual synapses, given N_p potential ones, is equal to the binomial probability of choosing N_s out of N_p:

$$B(N_s|N_p) = \frac{N_p!}{(N_p - N_s)!N_s!}\, p^{N_s}\,(1-p)^{N_p - N_s} \qquad [2]$$

Synaptically compatible neurons forming a given projection may share different numbers of potential synapses. This variability is captured by the distribution of potential synapse numbers, $P(N_p)$ (Fig. 1). The probability that a randomly chosen pair of synaptically compatible cells shares exactly N_s actual synapses can be obtained by calculating the average of $B(N_s|N_p)$ weighted with $P(N_p)$.

The above steps can be summarized into the following concise expression for the probability that a randomly selected pair of cells shares exactly N_s actual synapses:

$$A^{IM}(N_s) = (1-\kappa)\delta_{0,N_s} + \kappa \sum_{N_p=N_s}^{\infty} P(N_p)B(N_s|N_p) \qquad [3]$$

In this expression, $\delta_{0,Ns}$ is the Kronecker symbol, which equals 0 for all values of $N_s \geq 1$ and is 1 for $N_s = 0$. One may show that because the distribution of potential synapse numbers, $P(N_p)$, is normalized to one, the distribution of actual synapse numbers, $A^{IM}(N_s)$, is normalized to one as well.

Two experimental measures are typically reported regarding the connectivity between neurons. The first measure is the probability of connection, P_{con}. This is the probability that a randomly chosen pair of neurons is synaptically coupled. Within the model of independent synapse formation, P_{con} can be obtained by adding the probabilities for a randomly selected neuron pair to have one or more actual synapses:

$$P_{con}^{IM} = \sum_{N_s=1}^{\infty} A^{IM}(N_s) = \kappa \sum_{N_s=1}^{\infty} \sum_{N_p=N_s}^{\infty} P(N_p)B(N_s|N_p) \qquad [4]$$

The second experimental measurement is the distribution of actual synapse numbers between randomly selected, but synaptically connected, neurons, $A^{IM}(N_s \mid con)$. This conditional probability can be deduced from Bayes' rule:

$$A^{IM}(N_s|con) = \frac{A^{IM}(N_s, con)}{P_{con}^{IM}} \qquad [5]$$

Since we are only interested in the synaptically coupled neurons ($N_s \geq 1$), the joint probability $A^{IM}(N_s, con)$ can be replaced with $A^{IM}(N_s)$, and the distribution of synapse numbers for synaptically connected neurons reduces to:

$$A^{IM}(N_s|con) = \frac{\sum_{N_p=N_s}^{\infty} P(N_p)B(N_s|N_p)}{\sum_{N_s=1}^{\infty}\sum_{N_p=N_s}^{\infty} P(N_p)B(N_s|N_p)}, \qquad N_s \geq 1 \qquad [6]$$

The shape of $A^{IM}(N_s \mid con)$ depends only on a single parameter, p. In *Results*, Eq. **6** was used to generate $A^{IM}(N_s \mid con)$ for different values of p (Fig. 2).

Cooperative Synapse Formation Model. To provide a possible reconciliation between the numbers of actual and potential synapses for pairs of synaptically coupled neurons, we next considered a model of cooperative synapse formation (CM). In this model, the probability for synaptically coupled neurons to make N_s synapses (Eq. **6**) is modulated with a monotonically increasing sigmoidal function $f(N_s)$ (Eq. **1**).

$$A^{CM}(N_s|con) = \frac{1}{P_{con}^{CM}} f(N_s) \sum_{N_p=N_s}^{\infty} P(N_p)B(N_s|N_p), \qquad N_s \geq 1$$

$$P_{con}^{CM} = \sum_{N_s=1}^{\infty} f(N_s) \sum_{N_p=N_s}^{\infty} P(N_p)B(N_s|N_p) \qquad [7]$$

Again, P_{con} in these expressions is the probability of connection. The values of the model parameters p, N_s^c, and Δ, which result in $A^{CM}(N_s \mid con)$ that are statistically similar (at 5% significance level) to the experimentally observed distributions of synapse numbers are determined in *SI Text*. For further information, see Table S1.

ACKNOWLEDGMENTS. This work was supported by the National Institutes of Health Grants NS047138 and NS063494.

1. Shepherd GM, Stepanyants A, Bureau I, Chklovskii D, Svoboda K (2005) Geometric and functional organization of cortical circuits. *Nat Neurosci* 8:782–790.
2. Kalisman N, Silberberg G, Markram H (2005) The neocortical microcircuit as a tabula rasa. *Proc Natl Acad Sci USA* 102:880–885.
3. Lübke J, Roth A, Feldmeyer D, Sakmann B (2003) Morphometric analysis of the columnar innervation domain of neurons connecting layer 4 and layer 2/3 of juvenile rat barrel cortex. *Cereb Cortex* 13:1051–1063.
4. Jefferis GS, et al. (2007) Comprehensive maps of Drosophila higher olfactory centers: Spatially segregated fruit and pheromone representation. *Cell* 128:1187–1203.
5. Kisvárday ZF, et al. (1986) Synaptic targets of HRP-filled layer III pyramidal cells in the cat striate cortex. *Exp Brain Res* 64:541–552.
6. Stepanyants A, Chklovskii DB (2005) Neurogeometry and potential synaptic connectivity. *Trends Neurosci* 28:387–394.
7. Stepanyants A, Hof PR, Chklovskii DB (2002) Geometry and structural plasticity of synaptic connectivity. *Neuron* 34:275–288.
8. Trachtenberg JT, et al. (2002) Long-term in vivo imaging of experience-dependent synaptic plasticity in adult cortex. *Nature* 420:788–794.
9. Grutzendler J, Kasthuri N, Gan WB (2002) Long-term dendritic spine stability in the adult cortex. *Nature* 420:812–816.
10. Mizrahi A, Katz LC (2003) Dendritic stability in the adult olfactory bulb. *Nat Neurosci* 6:1201–1207.
11. Lee WC, et al. (2008) A dynamic zone defines interneuron remodeling in the adult neocortex. *Proc Natl Acad Sci USA* 105:19968–19973.
12. De Paola V, et al. (2006) Cell type-specific structural plasticity of axonal branches and boutons in the adult neocortex. *Neuron* 49:861–875.
13. Stettler DD, Yamahachi H, Li W, Denk W, Gilbert CD (2006) Axons and synaptic boutons are highly dynamic in adult visual cortex. *Neuron* 49:877–887.
14. Silberberg G, Gupta A, Markram H (2002) Stereotypy in neocortical microcircuits. *Trends Neurosci* 25:227–230.
15. Stepanyants A, et al. (2008) Local potential connectivity in cat primary visual cortex. *Cereb Cortex* 18:13–28.
16. Stepanyants A, Tamas G, Chklovskii DB (2004) Class-specific features of neuronal wiring. *Neuron* 43:251–259.
17. Kalisman N, Silberberg G, Markram H (2003) Deriving physical connectivity from neuronal morphology. *Biol Cybern* 88:210–218.
18. Amirikian B (2005) A phenomenological theory of spatially structured local synaptic connectivity. *PLoS Comput Biol* 1:E11.
19. Hellwig B (2000) A quantitative analysis of the local connectivity between pyramidal neurons in layers 2/3 of the rat visual cortex. *Biol Cybern* 82:111–121.
20. Binzegger T, Douglas RJ, Martin KA (2004) A quantitative map of the circuit of cat primary visual cortex. *J Neurosci* 24:8441–8453.
21. Feldmeyer D, Egger V, Lubke J, Sakmann B (1999) Reliable synaptic connections between pairs of excitatory layer 4 neurones within a single ''barrel'' of developing rat somatosensory cortex. *J Physiol* 521 (Pt 1):169–190.
22. Feldmeyer D, Lubke J, Silver RA, Sakmann B (2002) Synaptic connections between layer 4 spiny neurone-layer 2/3 pyramidal cell pairs in juvenile rat barrel cortex: Physiology and anatomy of interlaminar signalling within a cortical column. *J Physiol* 538 (Pt 3):803–822.
23. Markram H, Lubke J, Frotscher M, Roth A, Sakmann B (1997) Physiology and anatomy of synaptic connections between thick tufted pyramidal neurones in the developing rat neocortex. *J Physiol* 500 (Pt 2):409–440.
24. Ascoli GA (2006) Mobilizing the base of neuroscience data: The case of neuronal morphologies. *Nat Rev Neurosci* 7:318–324.
25. Thomson AM, Lamy C (2007) Functional maps of neocortical local circuitry. *Front Neurosci* 1:19–42.
26. Yu YC, Bultje RS, Wang X, Shi SH (2009) Specific synapses develop preferentially among sister excitatory neurons in the neocortex. *Nature* 458:501–504.
27. Le Be JV, Silberberg G, Wang Y, Markram H (2007) Morphological, electrophysiological, and synaptic properties of corticocallosal pyramidal cells in the neonatal rat neocortex. *Cereb Cortex* 17:2204–2213.
28. Frick A, Feldmeyer D, Helmstaedter M, Sakmann B (2008) Monosynaptic connections between pairs of L5A pyramidal neurons in columns of juvenile rat somatosensory cortex. *Cereb Cortex* 18:397–406.
29. Feldmeyer D, Roth A, Sakmann B (2005) Monosynaptic connections between pairs of spiny stellate cells in layer 4 and pyramidal cells in layer 5A indicate that lemniscal and paralemniscal afferent pathways converge in the infragranular somatosensory cortex. *J Neurosci* 25:3423–3431.
30. Stepanyants A, Martinez LM, Ferecsko AS, Kisvarday ZF (2009) The fractions of short- and long-range connections in the visual cortex. *Proc Natl Acad Sci USA* 106:3555–3560.
31. Laughlin SB, de Ruyter van Steveninck RR, Anderson JC (1998) The metabolic cost of neural information. *Nat Neurosci* 1:36–41.
32. Walsh MK, Lichtman JW (2003) In vivo time-lapse imaging of synaptic takeover associated with naturally occurring synapse elimination. *Neuron* 37:67–73.
33. Konur S, Rabinowitz D, Fenstermaker VL, Yuste R (2003) Systematic regulation of spine sizes and densities in pyramidal neurons. *J Neurobiol* 56:95–112.
34. Samsonovich AV, Ascoli GA (2006) Morphological homeostasis in cortical dendrites. *Proc Natl Acad Sci USA* 103:1569–1574.
35. Nagerl UV, Kostinger G, Anderson JC, Martin KA, Bonhoeffer T (2007) Protracted synaptogenesis after activity-dependent spinogenesis in hippocampal neurons. *J Neurosci* 27:8149–8156.
36. Matsumoto-Miyai K, et al. (2009) Coincident pre- and postsynaptic activation induces dendritic filopodia via neurotrypsin-dependent agrin cleavage. *Cell* 136:1161–1171.
37. Hebb DO (1949) *The Organization of Behavior: A Neuropsychological Theory* (Wiley, New York).
38. Markram H, Lubke J, Frotscher M, Sakmann B (1997) Regulation of synaptic efficacy by coincidence of postsynaptic APs and EPSPs. *Science* 275:213–215.
39. Lendvai B, Stern EA, Chen B, Svoboda K (2000) Experience-dependent plasticity of dendritic spines in the developing rat barrel cortex in vivo. *Nature* 404:876–881.
40. Feldman DE (2000) Timing-based LTP and LTD at vertical inputs to layer II/III pyramidal cells in rat barrel cortex. *Neuron* 27:45–56.
41. Helias M, Rotter S, Gewaltig MO, Diesmann M (2008) Structural plasticity controlled by calcium based correlation detection. *Front Comput Neurosci* 2:7.
42. Petersen CC, Hahn TT, Mehta M, Grinvald A, Sakmann B (2003) Interaction of sensory responses with spontaneous depolarization in layer 2/3 barrel cortex. *Proc Natl Acad Sci USA* 100:13638–13643.
43. Lübke J, Markram H, Frotscher M, Sakmann B (1996) Frequency and dendritic distribution of autapses established by layer 5 pyramidal neurons in the developing rat neocortex: comparison with synaptic innervation of adjacent neurons of the same class. *J Neurosci* 16:3209–3218.
44. Escobar G, Fares T, Stepanyants A (2008) Structural plasticity of circuits in cortical neuropil. *J Neurosci* 28:8477–8488.